

## SMALL PUNCH TESTS ON AUSTENITIC 316L STEEL SAMPLES PRE-EXPOSED IN LIQUID LEAD ENVIRONMENT

Valentin OLARU<sup>1</sup>, Vasile RADU<sup>2</sup>, Daniel DUPLEAC<sup>3</sup>

*Small Punch Tests were performed on samples made of austenitic 316L steel, pre-exposed in liquid lead, under temperature conditions of interest for the ALFRED demonstrator. The Small Punch Test produces a force-deflection curve, from which information about the elastoplastic deformation behaviour is extracted.*

*The test specimens were analyzed microscopically by considering the fracture surfaces and the specimens before and after exposure to liquid lead. The data obtained from the tests was processed in MATLAB to identify the material parameters for each sample. The liquid lead effect on candidate structural materials for the ALFRED demonstrator is highlighted.*

**Keywords:** liquid lead, Small Punch Test, 316L steel

### 1. Introduction

Early in the 1950s, studies and projects were started on the use of lead and Pb-Bi alloy (also known as Lead Bismuth Eutectic (LBE) as a cooling agent in fast nuclear reactors (LFR). There has been a lot of attention lately on the design of critical and subcritical reactors cooled by liquid lead (Pb) or lead-bismuth eutectic (LBE) in the context of developing Generation IV nuclear reactors. [1].

Currently, several experimental programs are being carried out worldwide to construct fast reactors with HLM cooling and recycle nuclear waste. These include the European Commission's four-year (2005–2009) integrated project for the TRANSmutation of High-Level Nuclear Waste in an Accelerator Driven System, IP-EUROTRANS [3] [4], and the United States' Advanced Fuel Cycle Initiative [2]. In addition, Europe is home to a large number of national-level initiatives, such as the GEDEPEON (Gestion de Déchets Radioactives par les Options Nouvelle) initiative in France and the MYRRHA project at SCK.CEN in Belgium. MYRRHA is being developed as an ADS to serve as a flexible neutron

<sup>1</sup> Researcher at Department of Nuclear Materials and Corrosion, Institute for Nuclear Research, Romania, e-mail: valentin.olaru@nuclear.ro

<sup>2</sup> Senior Researcher at Department of Nuclear Materials and Corrosion, Institute for Nuclear Research, Romania, e-mail: vasile.radu@nuclear.ro

<sup>3</sup> Professor at Faculty of Energy Engineering, Polytechnics University of Bucharest, Romania, e-mail: daniel.dupleac@upb.ro

source for research and development [5] [6] [7]. In addition, there are the South Korean HYPER (ADS) and PEACER programs [8] [9] [10], the Japanese program for the development of ADS and LFR [11] [12] [13] [14], and the Russian reactor programs BREST [15] and SVBR [16].

One of the six system concepts selected for future development under the Generation-IV Nuclear Energy Systems project is a class of Pb/LBE-cooled fast reactors (LFRs). A plethora of new applications for LFRs have been made possible by the properties of Pb/LBE, including the production of hydrogen, the processing of radioactive waste, and small modular reactors with long-lived cores that can provide heat and electricity to remote areas and/or underdeveloped nations.

This topic is of major interest at the Institute for Nuclear Research (RATEN ICN) in Romania, given the choice to design and construct the ALFRED experimental demonstrator, together with other support facilities, at this site.

The outcome of research into Europe's next generation of lead-cooled nuclear power reactors is the Advanced Lead Fast Reactor European Demonstrator (ALFRED). The primary objective of ALFRED and lead technology development is to preserve nuclear energy's significant role in the creation of a low-carbon, safe energy system in Europe. One of the projects supported by the EU's Strategic Energy Technology Plan (SET-Plan) and the European Sustainable Nuclear Industry Initiative (ESNII) to develop so-called fourth-generation fast neutron reactor technology is ALFRED, which promotes cooperation between research and industry [17].

Within the research community, the investigation of LFR candidate structural materials is of utmost importance. Liquid Metal Embrittlement (LME) [18], Liquid Metal Assisted Damage (LMAD) [19], and Environmentally Assisted Cracking (EAC) [20] are three categories for how liquid metals damage mechanical properties. It is a mechanical, physical-chemical process, and the interpretation of it is mostly dependent on the idea of wetting. Accurately characterizing the state of the surface in contact with the liquid metal at the right scale is crucial for a genuine comparison between these linked processes. The metallurgical and mechanical characteristics for LME, LMAD, or EAC failure could be more precisely determined once this critical stage is over.

In the present experimental study, the specific tests, called Small Punch Test (SPT), were carried out on samples made of austenitic 316L steel, pre-exposed in the molten lead for a long time. The samples were then subjected to SPTs under temperature conditions of interest to the ALFRED demonstrator. Microstructural analyses complement investigations at the microscopic scale.

## 2. Small Punch Test experiments

### 2.2 Description of test facility and specimens

The SPT-specific samples are in the shape of metal discs with a diameter of 10 mm and a thickness of 0.5 mm and are displayed in Fig. 2. Samples were cut from 316L steel plate (16.69% Cr, 10.26% Ni, 1.842% Mn, 2.075% Mo, 0.015% C, 0.027% P, 0.0028% S, 0.643% Si) by mechanical punching with a device specially designed for this operation (Fig. 2). Description of test facility and specimens.

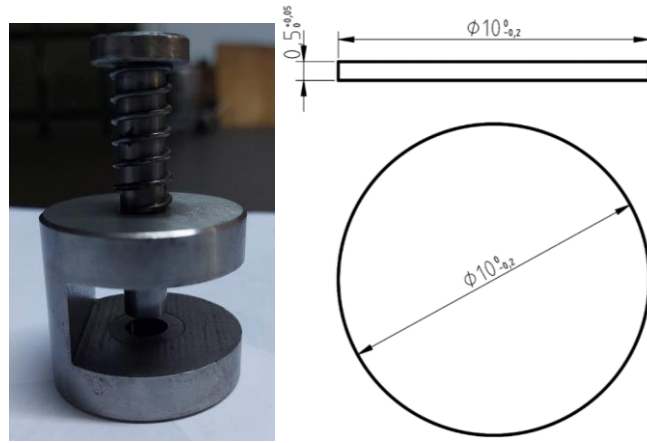


Fig. 2. Specimen punching device and sketch of the SPT sample of austenitic 316L steel.

In Fig. 3, the SPTs device is illustrated. It was developed at ICN Pitesti, Romania and it is used in conjunction with a Walter+Bai mechanical testing machine. The build-up of this device was based on scientific literature [1] and the ASTM standard for SPTs [20].

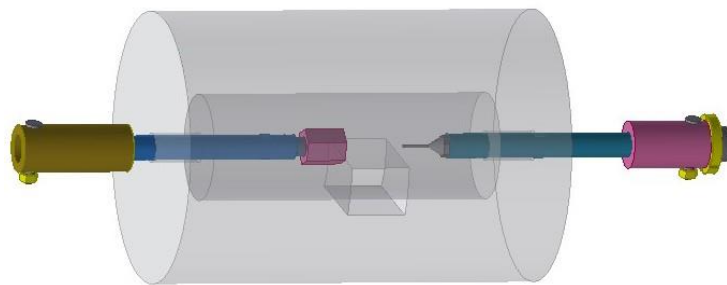


Fig. 3. Sketch of the SPT device inserted in the oven of the Walter+Bai installation.

Before testing or pre-exposure in a molten lead environment, SPT samples (Fig. 4) were polished on one side with 4000 ppm grit abrasive paper. This is necessary to obtain as flat a surface as possible and to minimize mechanical

stresses that may occur due to traces of surface machining of the sheet steel from which the samples were punched.



Fig. 4. 316L SPT samples polished with 4000 ppm grit abrasive paper.

This surface polishing also helps to more easily identify cracks and deformations that occur as a result of testing.

### 2.3. Exposure of samples in the liquid lead environment

To pre-expose the samples in liquid lead it was necessary to design a sample holder made of 316 steel and attach the samples using 316 steel wire (Fig. 5). This steel was chosen because of its known resistance to nickel leech in molten lead environments. This was necessary to not influence the liquid's chemistry during exposure.



Fig. 5. The 316L sample holder for pre-exposure in liquid lead environment.

The samples were therefore pre-exposed in a corrosion test facility in a liquid lead environment, which was set up to operate for an extended period under both atmospheric and temperature conditions.

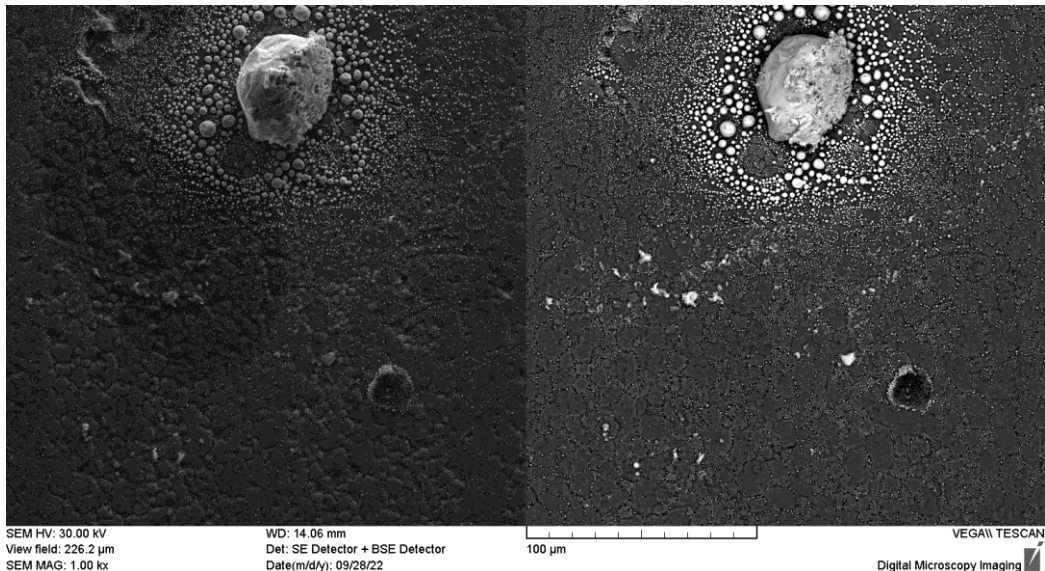
Pre-exposure was carried out in a molten lead environment with an oxygen concentration of about  $10^{-3}$  mass at  $400^{\circ}\text{C}$  for 200 hours. Samples after exposure treatment in molten lead are shown in Fig. 6.



Fig. 6. SPT samples after exposure to molten lead environment.

In Fig. 6, it can be seen that the samples once extracted from the liquid lead show considerable deposits of solidified lead on the surface. These samples must be cleaned with a special chemical solution designed to dissolve the lead on the surface without attacking the steel.

To have a reference to determine how well they were cleaned, the samples were observed under the electron microscope before being cleaned (Fig. 7).



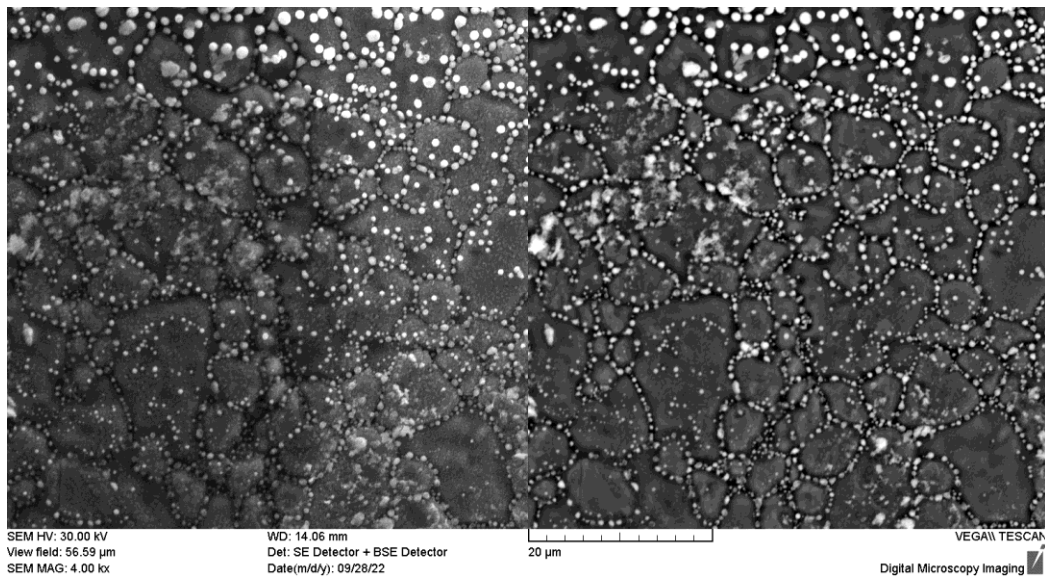


Fig. 7. SEM images of SPT samples after exposure in molten lead medium, secondary electrons (SE) (LEFT) and back-scattered electrons (BSE) (RIGHT) at X1000 (UP) and X4000 (DOWN) magnification.

The deposits of lead are observed on the surface of the samples in the form of grains with sizes from 50  $\mu\text{m}$  to 0.1  $\mu\text{m}$ . The smallest of these are concentrated at the grain boundaries of the steel in the substrate, which are now visibly eroded by contact with the liquid lead.

After cleaning the samples in acetic acid/oxygenated water solution (1:2), they were analysed again (Fig. 8). It is evident how effective the cleaning solution is.

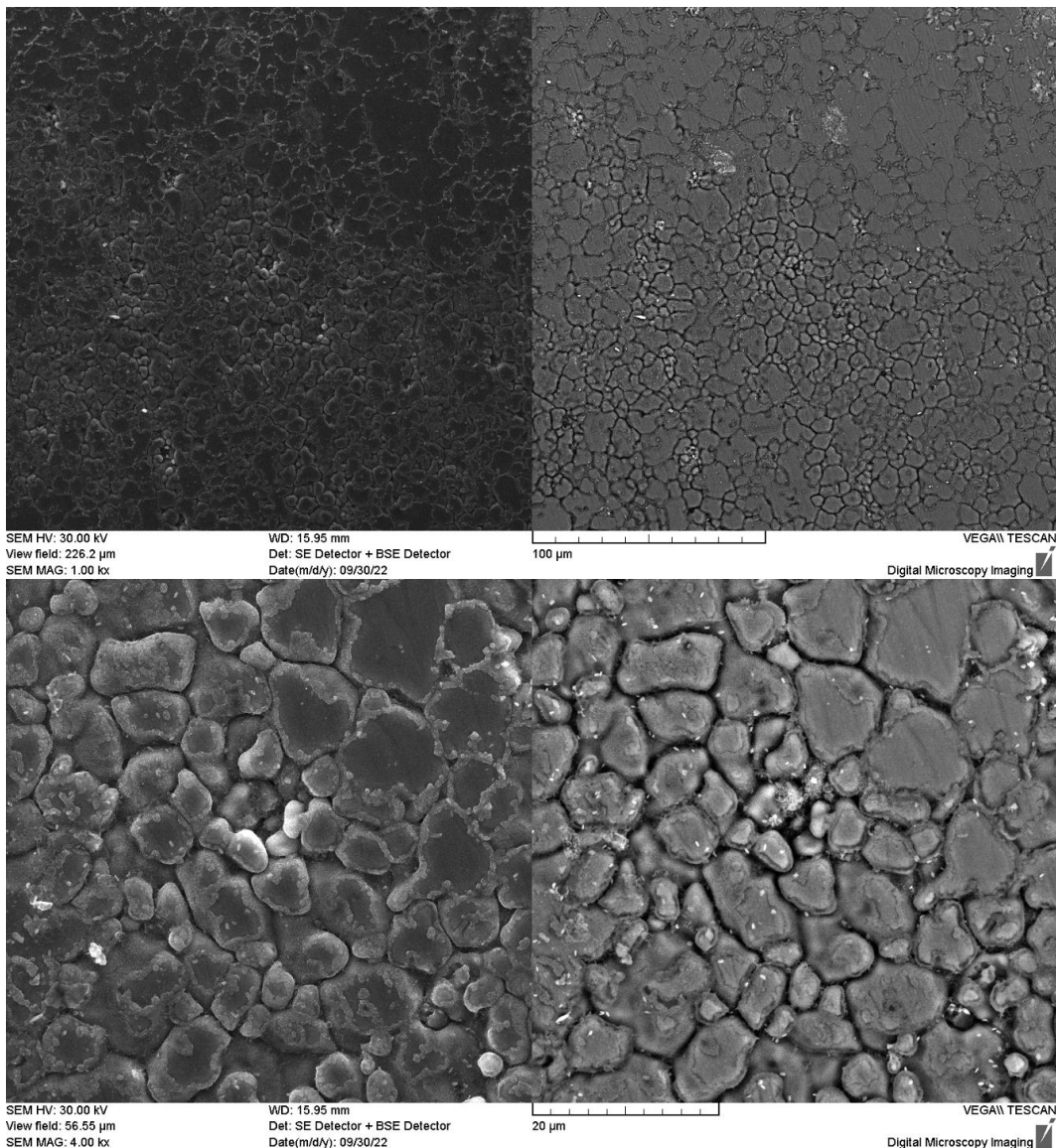


Fig. 8. SPT sample surface after lead cleaning, SE (LEFT) and BSE (RIGHT) at X1000 (UP) and X4000 (DOWN) magnification.

Before performing an analysis of the resulting images, another set of images was taken on a non-exposed sample to differentiate what the surface looked like before introduction into liquid lead (Fig. 9).

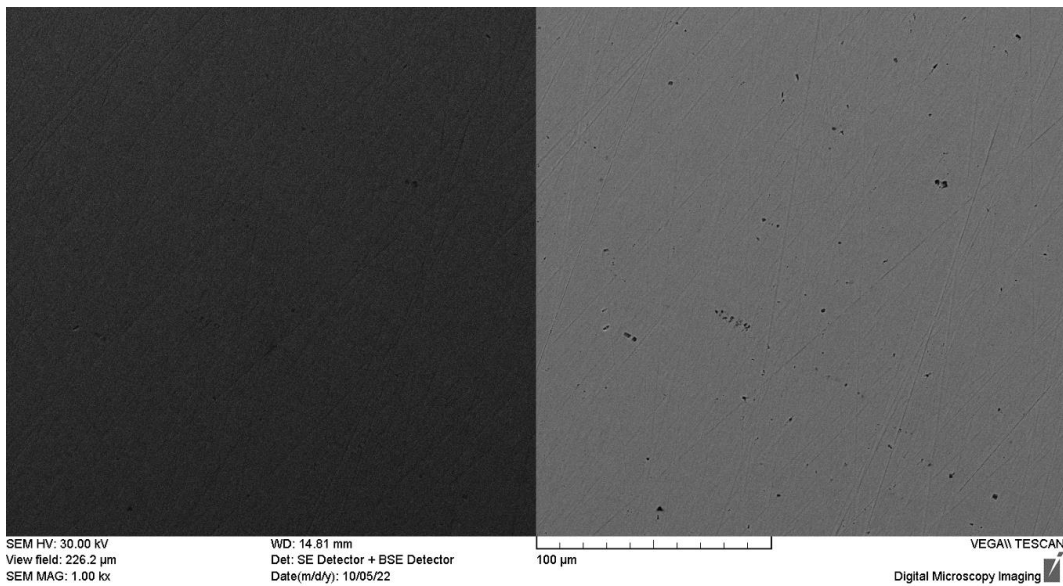


Fig. 9. SPT sample surface area before lead exposure, SE(LEFT) and BSE (RIGHT) at X1000 magnification.

From Fig. 8 and 9 we can see the corrosion factor of steel in contact with liquid lead. The metal grains on the surface of the sample were reduced such that voids in the material of the size of a few microns ( $\sim 4 \mu\text{m}$ ) were created. We don't yet know how this corrosion will affect the SPT test outcomes.

#### 2.4 The completed SPT test matrix

A total of 14 samples were selected to be tested in 4 test scenarios (room temperature - unexposed (as received) samples, room temperature - pre-exposed samples,  $400^\circ\text{C}$  - unexposed (as received) samples,  $400^\circ\text{C}$  - pre-exposed samples). The resulting test matrix is described in Table 1.

Table 1.

SPT test matrix - naming of samples and test scenarios.

Sample Name	23°C unexposed	23°C pre-exposed	400°C unexposed	400°C pre-exposed
RT AR 1	X			
RT AR 2	X			
RT AR 3	X			
RT AR 4	X			
RT PB 1		X		
RT PB 2		X		
RT PB 3		X		
RT PB 4		X		
400 AR 1			X	
400 AR 2			X	
400 AR 3			X	
400 PB 1				X
400 PB 2				X
400 PB 3				X

The tests were carried out on a Walter+Bai mechanical testing machine equipped with an oven to facilitate testing at 400°C. The speed at which the tungsten carbide ball indenter head was driven was 0.5 mm/min [20]. Both the displacement of the machine's hydraulic piston (recorded as "specimen deflection") and the force with which the ball pressed on the specimen surface were recorded.

The tests were performed without a strain gauge because the implementation of such a means of measurement is very difficult given the small proportions of the sample, the testing apparatus and the available space inside the oven. Fig. 10 displays the Force-Deflection diagrams that came from the tests.

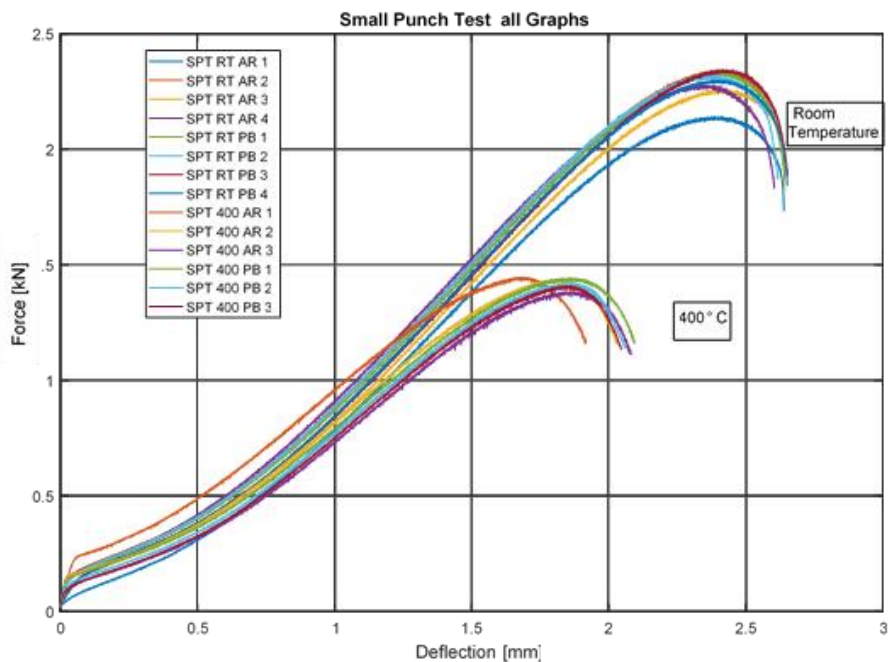


Fig. 10. Force-displacement (deflection) diagrams recorded during the SPT tests for the 4 test scenarios (room temperature - unexposed samples, room temperature - pre-exposed samples, 400°C - unexposed samples, 400°C - pre-exposed samples).

Analyzing the diagrams and taking into account the results of other international laboratories [1], we can conclude that the tested material (316L steel) had a ductile behavior both at room temperature and at 400°C. To verify this fact, the test samples were visualized on both sides to identify how cracking occurred (Fig. 11). In Fig. 12, the fracture surfaces are also displayed.

Four samples, one for each test scenario, were also chosen and sectioned by diameter, then embedded in epoxy resin to obtain images in cross-section (Fig. 13).



Fig. 11. Macrography of both surfaces for tested samples

The circular mode of fracture (circular cracks) can be observed, indicative of the ductility of the tested material, regardless of the temperature at which the test took place or sample treatment.

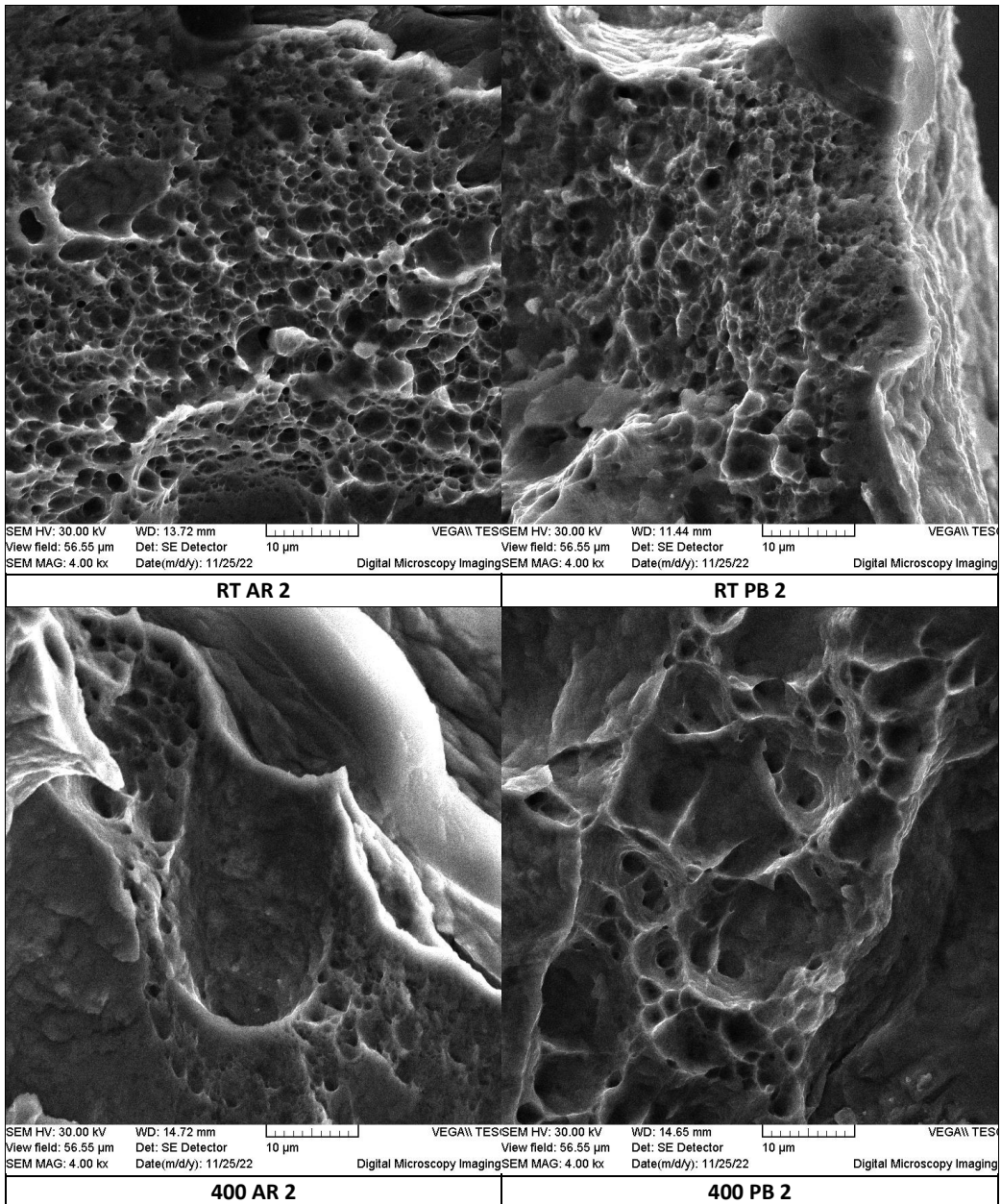


Fig. 12. SEM examinations of the fracture surfaces of samples chosen to symbolize every one of the four test situations.

The images of the fracture surfaces of the selected samples represent each of the four test scenarios highlight the ductile ("cone-cup") fracture pattern.

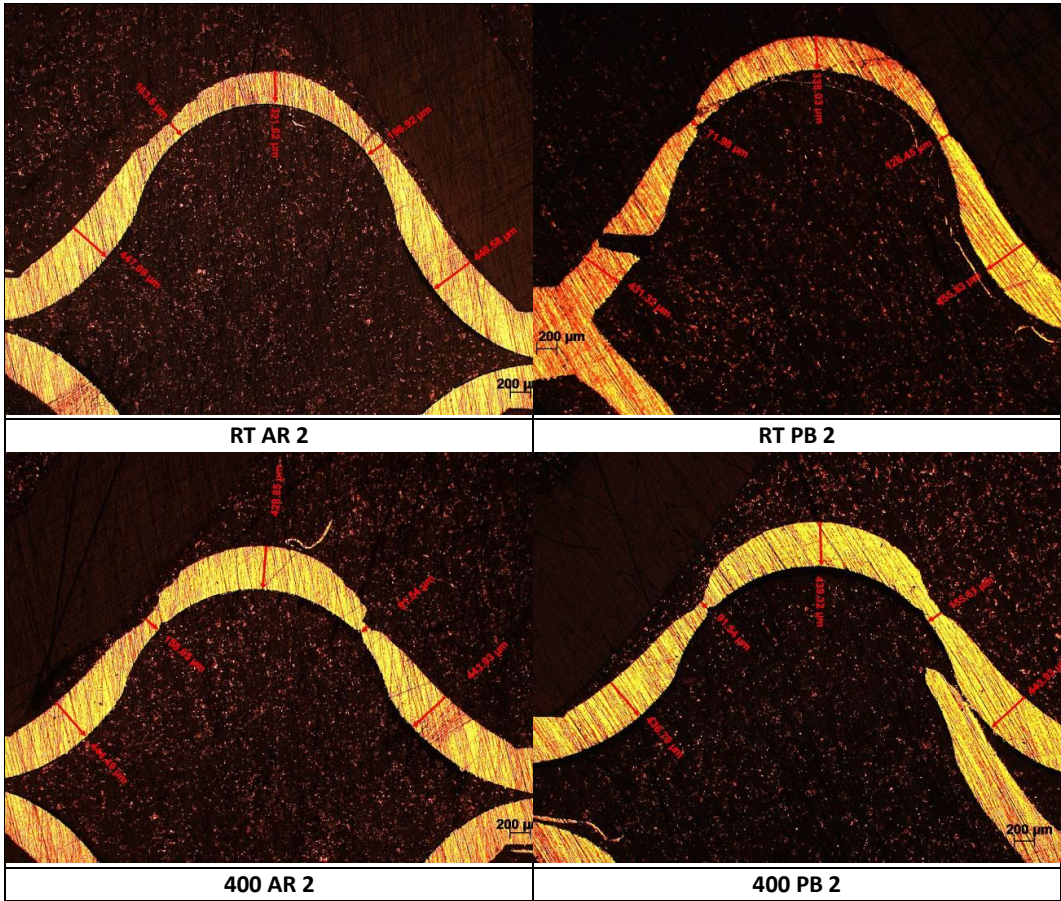


Fig. 13. The cross sections of the samples selected to represent each of the four test scenarios

We can see from Fig. 13 that the cross-sections of the selected samples show the typical  $45^\circ$  angle shearing and splitting mode of the ductile fracture.

Analyzing Fig. s 11, 12, 13, and together with the Force - Deflection graphs in Fig. 10 we can draw the final conclusion that the tested material (316L steel) had a ductile behavior both at room temperature and at  $400^\circ\text{C}$ , whether we refer to the unexposed samples or to the pre-exposed samples in molten lead.

## 2.5 Output parameters from Force-Deflection curves

As it can be seen in Fig. 10, the Force-Deflection curves resulting from the SPT tests are grouped in two areas (room temperature and  $400^\circ\text{C}$ ). A clear difference between the curves of unexposed and pre-exposed samples at a given temperature is difficult to see, as they are very close in terms of maximum force.

MATLAB was utilized to process the test data and determine the material properties as mentioned in the reference [20] and recalled as such:

- $F_e$  [N] - force defining the shift from linearity to the stage connected to the yield zone spreading throughout the thickness of the specimen (plastic bending stage).
- $F_m$  [N] - maximal force measured while doing the SP test.
- $u_m$  [mm] - specimen deflection in relation to the strongest force  $F_m$ .
- $u_f$  [mm] - specimen deflection in relation to a 20% force decrease with respect to  $F_m$ , i.e.,  $F_f = 0.8 F_m$ .
- $E_{SP}$  [J] - Calculated under the area under the  $F-u$  curve up to  $u_f$ , SP fracture energy.
- $E_m$  [J] - Total SP energy (plastic + elastic) up to  $u_m$ , as determined by calculating the area under the  $F-u$  curve.
- $E_{PL}$  [J] - Calculated from the area under the  $F-u$  curve up to  $u_m$ , SP plastic energy.

The 14 curves were analysed, and one curve (RT AR 2 - unexposed sample tested at room temperature) was chosen to exemplify here the steps to find the parameters described above. Fig. 14 illustrates how the parameter values  $F_m$ ,  $F_f$ ,  $u_m$  and  $u_f$  were found.

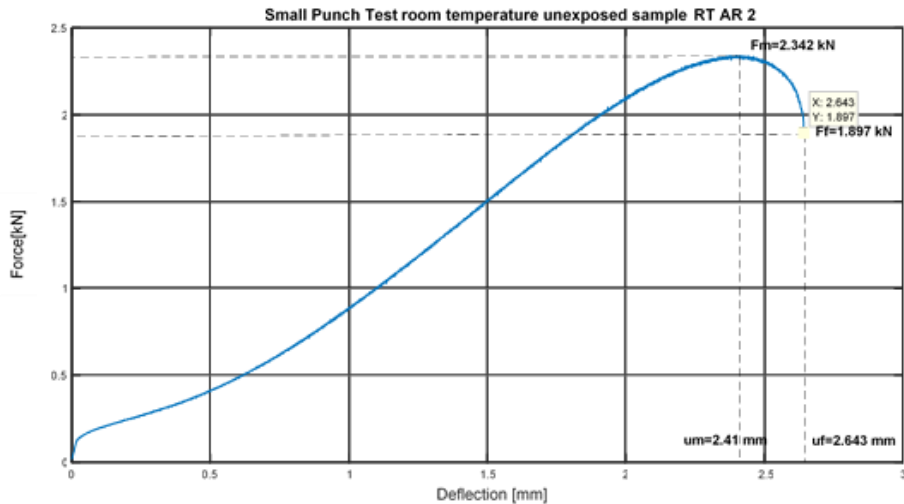
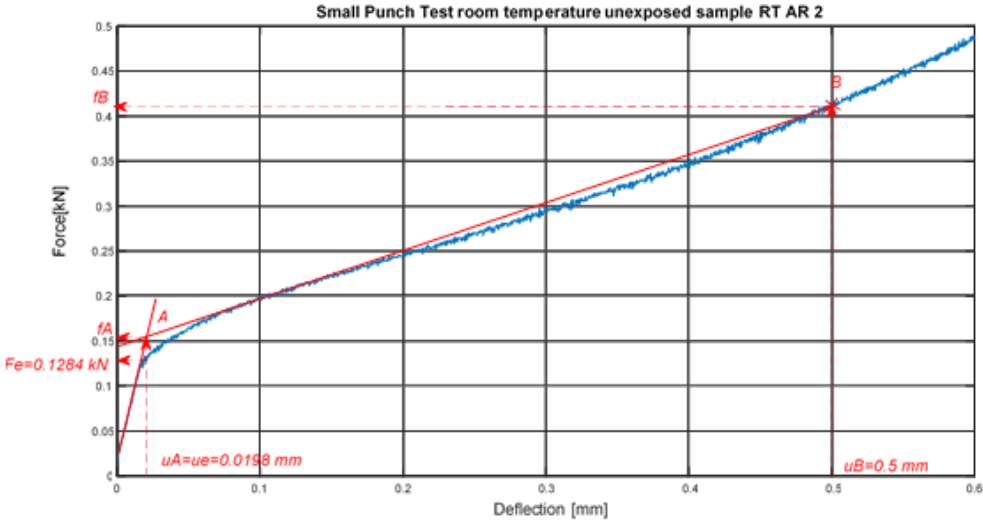


Fig. 14. Determination of  $F_m$ ,  $F_f$ ,  $u_m$  and  $u_f$  parameters for RT AR 2 sample

The next step is to approximate the Force-deflection curve in the transition zone from elastic to elastoplastic with two intersecting straight lines. Both the process and the parameter determination of  $F_e$  and  $u_e$  is shown in Fig. 15.

Fig. 15. Determination of  $F_e$  and  $u_e$  parameters for RT AR 2 sample.

The SPT results for all tested samples are mentioned in Table 2.

Table 2.  
Results of analysis of the SPT tests

Nr. Proba	$F_e$ (kN)	$u_e$ (mm)	$F_m$ (kN)	$u_m$ (mm)	$F_r=0.8F_m$ (kN)	$u_r$ (mm)	$E_{SP}$ (J) (u <sub>r</sub> )	$E_m$ (J) (u <sub>m</sub> )	$E_{PL}$ (J) (u <sub>e</sub> -u <sub>m</sub> )
RT AR 1	0,1403	0,0193	2,279	2,379	1,832	2,605	3,2978	2,8082	2,8065
RT AR 2	0,1284	0,0198	2,342	2,41	1,897	2,643	3,393	2,8688	2,8671
RT AR 3	0,1186	0,0441	2,257	2,414	1,821	2,642	3,2112	2,7131	2,7097
RT AR 4	0,1366	0,0178	2,284	2,347	1,835	2,604	3,2978	2,7365	2,735
RT PB 1	0,125	0,0192	2,337	2,41	1,874	2,642	3,3534	2,835	2,8334
RT PB 2	0,1128	0,018	2,324	2,369	1,872	2,616	3,3249	2,7701	2,7688
RT PB 3	0,1155	0,0444	2,347	2,452	1,886	2,652	3,3283	2,8809	2,8776
RT PB 4	0,1219	0,0534	2,302	2,381	1,845	2,652	3,3144	2,7134	2,7093
400 AR 1	0,2105	0,045	1,444	1,704	1,16	1,916	1,6898	1,4017	1,3961
400 AR 2	0,1528	0,02565	1,44	1,815	1,161	2,029	1,6695	1,377	1,3747
400 AR 3	0,09375	0,0148	1,384	1,847	1,112	2,081	1,605	1,2974	1,2965
400 PB 1	0,1373	0,02665	1,445	1,864	1,164	2,096	1,7354	1,418	1,4158
400 PB 2	0,1074	0,01505	1,421	1,871	1,141	2,061	1,6417	1,3889	1,3879
400 PB 3	0,08091	0,01375	1,41	1,858	1,136	2,047	1,5903	1,3401	1,3393

From the analysis of the recorded curves in Fig. 10, there is no easy-to-see difference between the behaviour of unexposed (untreated) samples and the behaviour of pre-exposed samples. However, we can draw comparative plots between the mean energies for unexposed and pre-exposed samples. These plots are shown in Fig. 16.

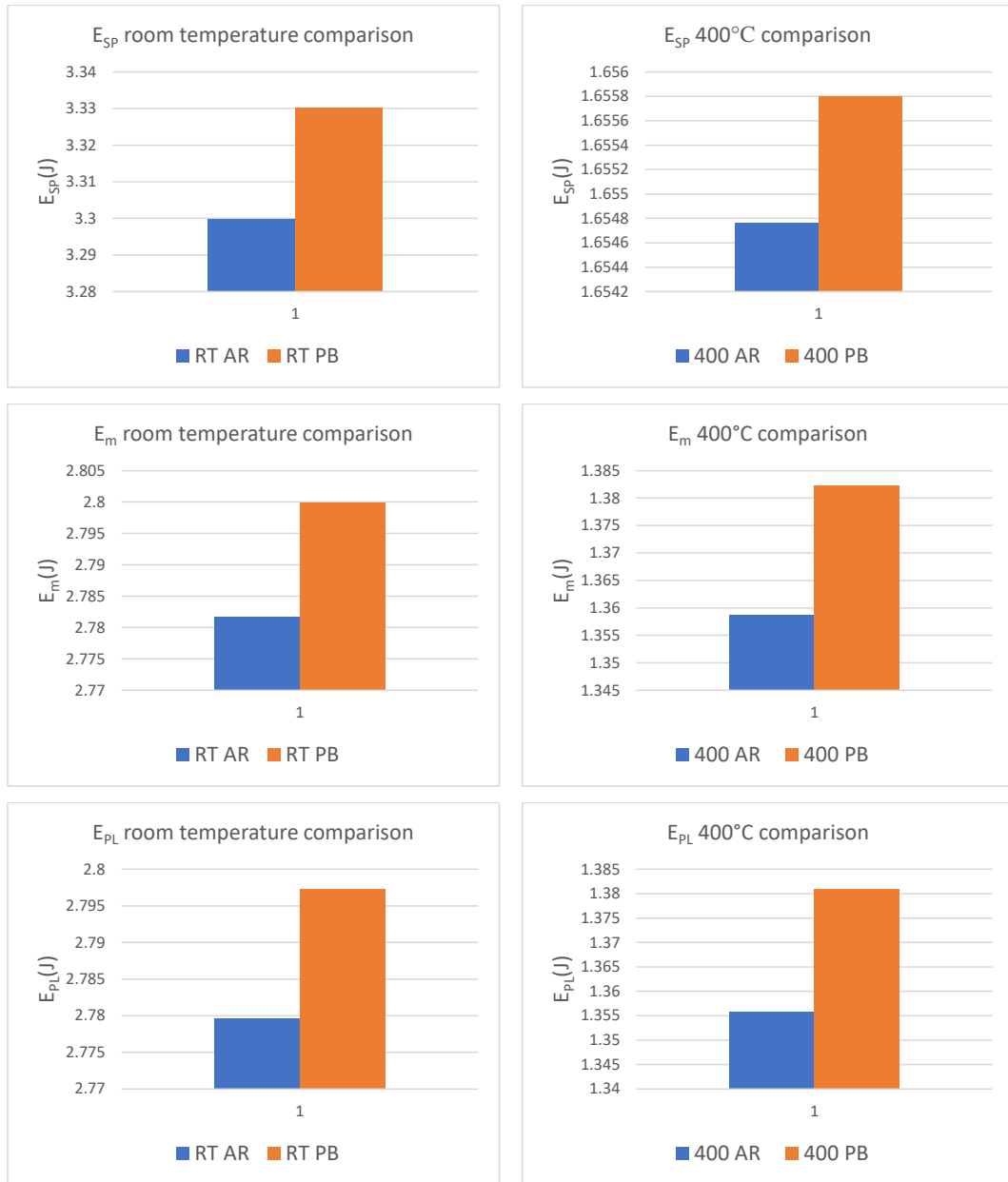


Fig. 16. Comparative charts between the mean energies for unexposed and pre-exposed samples at room temperature and 400°C.

From the comparative plots, it can be concluded that, although the differences are very small, higher strain energies were obtained from the tests of the pre-exposed samples in lead than for the unexposed ones. If we take into

account the images in Figs. 7 and 8, where the corrosive influence of lead on the surfaces of pre-exposed samples was highlighted, the higher specific energies determined on the pre-exposed samples contribute to the fact that the heat treatment upon lead exposure of the samples can counterbalance the possible corrosion-induced embrittlement. This may become significant for long periods of pre-exposure in molten lead media, provided oxygen is controlled, which in turn may increase the incidence of oxidation embrittlement.

### 3. Conclusions

Small Punch Test tests were performed on samples made of austenitic 316L steel, pre-exposed in molten lead, which were then subjected to SPT tensile tests under temperature conditions of interest to the ALFRED demonstrator.

The conclusions of the present work are:

- A total of 14 samples were selected to perform the SPT in 4 test scenarios (room temperature - unexposed samples, room temperature - pre-exposed samples, 400°C - unexposed samples, 400°C - pre-exposed samples).
- Analyzing the Force-displacement (deflection) diagrams we can conclude that the tested material (316L steel) had a ductile behaviour both at room temperature and at 400°C. Also, microscopic analysis revealed corrosion of samples in contact with liquid lead and ductile fracture of all samples following SPT tests.
- From the analysis of the Force-displacement diagrams, there is no clear difference between the behaviour of the unexposed samples and the behaviour of the pre-exposed samples. From the comparative charts of the energies resulting from the SPT one can conclude that, although the differences are very small, somewhat higher strain energies were obtained from the tests of the pre-exposed samples in lead than for the unexposed ones.
- If we consider the images from which the corrosive influence of lead on the surfaces of the pre-exposed specimens was evidenced, the higher specific energies determined on the pre-exposed specimens confirm that the heat treatment upon lead exposure of the specimens can counterbalance the possible corrosion-induced embrittlement.

Further activities in the research programs which are in progress at RATEN ICN, in the field of Generation IV nuclear reactors, will be focused on investigating the influence of exposure in liquid lead environment on the mechanical properties of 316L stainless steel specimens. These tests will contribute to the study of the effect of liquid lead corrosiveness on the candidate structural materials for Generation IV nuclear reactors.

## R E F E R E N C E S

- [1] OECD-NEA, Handbook on lead-bismuth eutectic alloy and lead properties, materials compatibility, thermal-hydraulics and technologies, Issy-les-Moulineaux, France: OECD-NEA 6195, 2007.
- [2] Report to Congress on Advanced Fuel Cycle Initiative: The Future Path for Advanced Spent Fuel Treatment and Transmutation Research (2003), US DOE, Office of Nuclear Energy, Science and Technology.
- [3] Integrated Project EUROpean Research Programme for the TRANSmutation of High Level Nuclear Waste in an Accelerator Driven System, EUROTRANS (2004), EC project No. FI6W-CT-2004-516520.
- [4] Knebel, J.U., et al. (2005), "Overview on Integrated Project EUROTRANS: EUROpean Research Programme for the TRANSmutation of High Level Nuclear Waste in an Accelerator Driven System", 3rd Annual Idaho ADSS Experiments Workshop, Pocatello, ID, 1-2 June 2005.
- [5] Abderrahim, H. Aït, et al. (2001), "MYRRHA: A Multipurpose Accelerator Driven System for Research & Development", Nuclear Instruments & Methods in Physics Research, A 463, 487-494.
- [6] Abderrahim, H. Aït (2005a), "MYRRHA: A Multipurpose ADS for R&D, Progress Report at End 2004", ICONE 13, Beijing.
- [7] Abderrahim, H. Aït, D. de Bruin (2005b), MYRRHA, a Future for Nuclear Research. Pre-design (DRAFT-2) Report, H. Aït Abderrahim, D. de Bruin (Eds.), SCKCEN report, Mol, Belgium.
- [8] Hwang, I.S., S.H. Jeong, B.G. Park, W.S. Yang, K.Y. Suh, C.H. Kim (2000), "The Concept of Proliferation-resistant, Environment-friendly, Accident-tolerant, Continual and Economical Reactor (PEACER)", Progress in Nuclear Energy, Vol. 37, No. 1-4, pp. 217-222.
- [9] Song, T.Y., et al. (2004), "HYPER Project", Proceedings of OECD/NEA 4th International Workshop on Utilisation and Reliability of High Power Proton Accelerators, Daejeon, Korea, 16-19 May 2004.
- [10] Park, W.S., et al. (1996), Development of Nuclear Transmutation Technology, KAERI/RR-1702/96; Proceedings of International Conference on Heavy Liquid Metal Coolants in Nuclear Engineering, Vol. 1, 2, p. 824, 5-9 Oct. 1998, Obninsk, IPPE.
- [11] Sasa, T., et al. (2004), "Research and Development on Accelerator-driven Transmutation System at JAERI", Nuclear Engineering and Design, 230, pp. 209-222.
- [12] Takahashi, M., et al. (2004), "Design and Experimental Study for Development of Pb-Bi Cooled Direct Contact Boiling Water Small Fast Reactor (PBWFR)", Proc. of ICAPP'04, Pittsburgh, PA, USA, 13-17 June 2004, paper 4058.
- [13] Oigawa, H., et al. (2004), "R&D Activities on Accelerator-driven Transmutation System in JAERI", OECD/NEA 8th Information Exchange Meeting on Actinide and Fission Product Partitioning & Transmutation, Las Vegas, Nevada, USA, 9-11 November 2004.
- [14] Mukaiyama, T. (1999), OMEGA Programme in Japan and ADS Development at JAERI, IAEA TECDOC--1365, pp. 153-165.
- [15] Filin, A.I., et al. (2000), Design Features of BREST Reactors and Experimental Work to Advance the Concept of BREST Reactors, IAEA-TECDOC 1348, pp. 36-47, 23-27 October 2000.
- [16] Stepanov, V.S., et al. (1998), SVBR-75: A Reactor Module for Renewal of WWER-440 Decommissioning Reactors – Safety and Economic Aspects, IAEA TECDOC 1056, pp. 165-176, November 1998.

- [17] A. Alemberti, et al. (2015), ALFRED and the Lead Technology Research Infrastructure, European Research Reactor Conference (RRFM) 2015 Conference Proceedings.
- [18] *M.H. Kamdar*, “Embrittlement by Liquid Metals”, *Prog. Mater. Sci.*, 1973, 15, pp. 289-372.
- [19] *S. Maloy*, Handbook on Lead-bismuth Eutectic Alloy and Lead Properties, Materials Compatibility, Thermal-hydraulics and Technologies, LANL, United States, 2015.
- [20] ASTM E3205-20 « Standard Test Method for Small Punch Testing of Metallic Materials », 2020.